

# Assembly and Disassembly of Langmuir–Blodgett Films on Poly[1-(trimethylsilyl)-1-propyne]: The Uniqueness of Calix[6]arene Multilayers as Permeation-Selective Membranes

Robert A. Hendel, Eisaku Nomura, Vaclav Janout, and Steven L. Regen\*

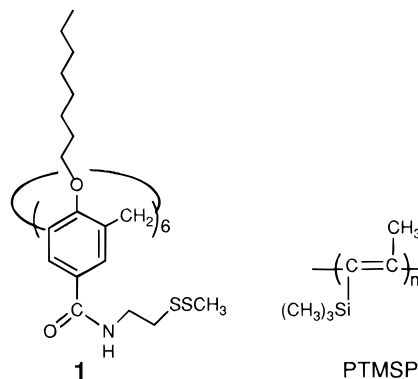
Contribution from the Department of Chemistry and Zettlemoyer Center for Surface Studies, Lehigh University, Bethlehem, Pennsylvania 18015

Received March 27, 1997<sup>⊗</sup>

**Abstract:** A series of calix[6]arene-based surfactants have been synthesized, which contain amide oxime head groups on their upper rim and 5,5-dimethylhexyl (**I**), *n*-octyl (**II**), *n*-dodecyl (**III**), and *n*-hexadecyl (**IV**) groups on their lower rim. Composite membranes that were fabricated from Langmuir–Blodgett (LB) multilayers derived from each surfactant plus poly[1-(trimethylsilyl)-1-propyne] (PTMSP) cast film showed a significant increase in their selectivity toward helium and nitrogen, relative to bare PTMSP. In sharp contrast, analogous composites that were prepared with LB multilayers of conventional single chain surfactants [arachidic acid (**AA**), cadmium arachidate (**AA**/Cd<sup>2+</sup>), and stearoamideoxime (**SA**)] exhibited permeation properties that were identical with those of bare PTMSP. When a polymeric surfactant [poly(1-octadecene-*co*-maleic anhydride), **POM**] was used for LB film construction, a modest increase in selectivity was observed. These findings, together with an analysis of representative composites by X-ray photoelectron spectroscopy, provide compelling evidence for the presence of intact, calix[6]arene-based LB assemblies on the surface of PTMSP; with the conventional single chain surfactants, however, disassembly and absorption into the bulk phase of the support is favored. The results of this study highlight the need for having individual surfactant molecules span individual pores on the surface of the support and strong intermolecular forces between neighboring surfactants to produce relatively defect-free LB films.

## Introduction

We have previously shown that Langmuir–Blodgett (LB) films derived from certain calix[6]arenes exhibit significant permeation selectivity when supported on poly[1-(trimethylsilyl)-1-propyne] (PTMSP).<sup>1–3</sup> For example, we have shown that multilayers of **1**, deposited onto PTMSP cast film, are much more permeable toward helium than nitrogen.<sup>1</sup> The fact that this selectivity is greater than what would be expected based on Graham's law has provided compelling evidence that the pores through which these permeants pass are of molecular dimensions. Although the precise nature of these pores remains to be established, our working hypothesis has been that the “molecular pores” of the calix[6]arenes are of primary importance. In principle, transient gaps between the calix[6]arenes (resulting from thermal motion), as well as defects, may also contribute to the overall pore structure of such assemblies.<sup>4</sup> Of special significance is the fact that these membranes represent the only known examples of LB films in which permeation through the assemblies (as opposed to defects) represents the major diffusional pathway.<sup>5–11</sup>



Our success in fabricating permeation-selective LB films from calix[6]arenes was found to be critically dependent upon the specific support material that was used.<sup>2</sup> Thus, when microporous PTMSP cast films were employed, significant selectivity was observed; when macroporous polymer supports were used (i.e., Celgard and Nuclepore membranes), however, no significant selectivity was detected. Our presumption has been that the relatively contiguous surface of PTMSP film minimizes the formation of defects within the LB overlayer. Specifically, we hypothesized that by minimizing the need for “bridging the gaps” on the surface of the support, the LB film is more likely to remain intact. Recent positron annihilation studies of PTMSP indicate that these cast films contain pores that are ca. 10 Å in diameter.<sup>12</sup> Given the size of the calix[6]arene framework (a cylindrical conformation maintains an outer diameter of ca. 14 Å), one would expect that *individual calix[6]arene-based surfactants should be able to span individual pores on the surface of PTMSP*. In contrast, Celgard [a

<sup>⊗</sup> Abstract published in *Advance ACS Abstracts*, July 1, 1997.

(1) Conner, M. D.; Janout, V.; Regen, S. L. *J. Am. Chem. Soc.* **1993**, *115*, 1178.

(2) Conner, M. D.; Janout, V.; Kudelka, I.; Dedek, P.; Zhu, J.; Regen, S. L. *Langmuir* **1993**, *9*, 2398.

(3) Dedek, P.; Webber, A. S.; Janout, V.; Hendel, R. A.; Regen, S. L. *Langmuir* **1994**, *10*, 3943.

(4) Stern, S. A. *J. Membr. Sci.* **1994**, *94*, 1.

(5) Rose, G. D.; Quinn, J. A. *Science* **1968**, 636.

(6) Rose, G. D.; Quinn, J. A. *J. Colloid Interface Sci.* **1968**, *27*, 193.

(7) Albrecht, O.; Laschewsky, A.; Ringsdorf, H. *Macromolecules* **1984**, *17*, 937.

(8) Stroeve, P.; Spooner, G. J. R.; Bruinsma, P. J.; Coleman, L. B.; Erdelen, C.; Ringsdorf, H. *Am. Chem. Soc., Symp. Ser.* **1990**, *447*, 177.

(9) Kigashi, N.; Kunitake, T.; Kajiyama, T. *Polym. J.* **1987**, *19*, 289.

(10) Stroeve, P.; Coelho, M. A. N.; Dong, S.; Lam, P.; Coleman, L. B.; Fiske, T. G.; Ringsdorf, H.; Schneider, J. *Thin Solid Films* **1989**, *180*, 291.

(11) Stroeve, P.; Bruinsma, P. J. *Thin Solid Films* **1994**, *244*, 958.

(12) Yampol'ski, Y. P.; Shantorovich, V. P.; Cherrnyakovski, F. P.; Kornilov, A. I.; Plate, N. A. *J. Appl. Polym. Sci.* **1993**, *47*, 85.

stretched form of poly(propylene)] would require ca.  $6 \times 10^3$  calix[6]arenes to cover a rectangular pore that is typically  $2000 \text{ \AA} \times 500 \text{ \AA}$ ; for Nuclepore membranes that contain  $300 \text{ \AA}$  diameter cylindrical pores, ca. 400 calix[6]arenes would be needed.

Although our studies to date have demonstrated the utility of PTMSP as support material for LB films, the question of uniqueness of the calix[6]arenes, themselves, has not been firmly established. In particular, no direct comparisons have yet been made between calix[6]arene-based LB films and those made from conventional single chain or polymeric surfactants. Moreover, the question of whether or not the permeation properties of calix[6]arene-based LB films can be fine-tuned by altering their molecular structure and/or composition remains unanswered. The primary aim of the work that is described herein was to address both of these issues.<sup>13</sup>

## Experimental Section

**General Methods.** Unless stated otherwise, all reagents and chemicals were obtained from commercial sources and used without further purification. EMS silica gel 60 was used for column chromatography; preparative thin layer chromatography employed EM Science silica gel 60 F-254. Detection by TLC was made by a combination of 10% sulfuric acid in water,  $I_2$ , and UV (254 and 365 nm). House-deionized water was purified with a Millipore Milli-Q-filtering system containing one carbon and two ion-exchange stages. Chloroform and methanol, which were used as spreading solvents for monolayer formation, were HPLC grade (Burdick and Jackson, Baxter). All  $^1\text{H}$  NMR spectra were recorded on a Bruker 360-MHz instrument; chemical shifts are reported in ppm and were referenced to residual solvents. High resolution mass spectra (fast atom bombardment) were obtained at the Mass Spectrometry Facility of the University of California, Riverside. Elemental analyses were obtained from Midwest Microlab (Indianapolis, IN). 37,38,39,40,41,42-Hexahydroxycalix[6]arene and 37,38,39,40,41,42-hexakis(1-octyloxy)calix[6]arene were prepared by using procedures similar to those that have been previously described.<sup>14</sup> All monolayer measurements, film casting, and membrane fabrications were performed in a clean room that was maintained under a positive pressure via a Hepa filtration system. The polymeric surfactant, poly(1-octadecene-*co*-maleic anhydride) (POM), was obtained from a commercial source (Polysciences, MW 30 000 to 50 000) and was used as received. Eicosanoic (arachidic) acid was purchased from Aldrich Chemical Co.

**5,5-Dimethylhexyl-1-methanesulfonate.** A solution of 5.00 g (69.3 mmol) of 3-buten-1-ol in 30 mL of anhydrous pyridine was stirred and cooled in an ice bath.

*p*-Toluenesulfonyl chloride (16.5 g, 86.6 mmol) was then added in small portions, while maintaining the temperature of the mixture at 0–5 °C. The resulting slurry was allowed to stand for 16 h, while keeping the temperature below 10 °C, and then poured into 100 g of ice water. Subsequent extraction with  $\text{CH}_2\text{Cl}_2$  ( $4 \times 30 \text{ mL}$ ), washing of the combined extract with 1 M sulfuric acid ( $4 \times 30 \text{ mL}$ ), 10 mL of saturated  $\text{NaHCO}_3$ , and water ( $2 \times 10 \text{ mL}$ ), drying (anhydrous  $\text{MgSO}_4$ ), and concentration under reduced pressure afforded 14.4 g (92%) of 3-butenyl-1-*p*-toluenesulfonate as a colorless oil having  $^1\text{H}$  NMR ( $\text{CDCl}_3$ )  $\delta$  2.34–2.40 (m, 2 H), 2.42 (s, 3 H), 4.04 (t, 2 H), 5.02–5.07 (m, 2 H), 5.61–5.68 (m, 1 H), 7.32 (d, 2 H), 7.76 (d, 2 H).

A dispersion of 8.96 g (100.0 mmol) of  $\text{CuCN}$  in 140 mL of anhydrous THF was stirred under a nitrogen atmosphere and cooled to –78 °C. To this dispersion was added, dropwise, 118 mL of 1.7 M  $(\text{CH}_3)_3\text{CLi}$  in pentane over the course of 1 h. The mixture was then stirred and warmed, gradually, until a homogeneous orange solution

appeared (at ca. –10 °C), and then cooled to –78 °C. To this cuprate solution was added 20 mL of a THF solution that contained 9.05 g (40.0 mmol) of 3-butenyl-1-*p*-toluenesulfonate over a period of 30 min. The mixture was stirred for 3 h while the temperature was gradually raised to –10 °C, and then poured into 100 mL of a saturated solution of  $\text{NH}_4\text{Cl}$  that was cooled to 0 °C and stirred for 10 min. The organic layer was separated, washed with saturated  $\text{NH}_4\text{Cl}$  until appearing colorless, further washed with saturated  $\text{NaCl}$ , and then dried over anhydrous  $\text{MgSO}_4$ . Concentration and purification by distillation afforded 3.05 g (68%) of 5,5-dimethyl-1-hexene having bp 82 °C;  $^1\text{H}$  NMR ( $\text{CDCl}_3$ )  $\delta$  0.87 (s, 9 H), 1.23–1.27 (m, 2 H), 1.96–2.03 (m, 2 H), 4.88–5.01 (m, 2 H), 5.76–5.87 (m, 1 H).

To a mixture of 0.95 g (25 mmol) of  $\text{NaBH}_4$  and 1.32 g (5 mmol) of 18-crown-6 in 50 mL of anhydrous THF was added 0.77 g (5 mmol) of  $\text{TiCl}_3$ .<sup>15</sup> After the mixture was stirred for 1 h at 25 °C under a nitrogen atmosphere, a solution made from 2.86 g (25 mmol) of 5,5-dimethyl-1-hexene and 10 mL of anhydrous THF was added in a dropwise manner. The mixture was then stirred for 18 h at 25 °C, followed by sequential addition (dropwise) of 17.5 mL of 25 wt %  $\text{CH}_3\text{ONa}$  in  $\text{CH}_3\text{OH}$  (w/w) and 45 mL of 30%  $\text{H}_2\text{O}_2$ . The mixture was stirred for an additional 1 h at room temperature and extracted with  $\text{CH}_2\text{Cl}_2$  ( $3 \times 50 \text{ mL}$ ), and the combined organic extract was washed with water ( $3 \times 30 \text{ mL}$ ) and dried (anhydrous  $\text{MgSO}_4$ ). Removal of solvent under reduced pressure afforded 2.85 g (88%) of 5,5-dimethyl-1-hexanol as a colorless oil having  $^1\text{H}$  NMR ( $\text{CDCl}_3$ )  $\delta$  0.85 (s, 9 H), 1.14–1.19 (m, 2 H), 1.27–1.29 (m, 2 H), 1.35 (s, 1 H), 1.50–1.54 (m, 2 H), 3.63 (t, 2 H). HRMS for  $\text{MNH}_4^+(\text{C}_8\text{H}_{22}\text{NO})^+$ : calcd, 148.1701; found, 148.1691.

To 50 mL of cooled (–10 °C) anhydrous  $\text{CH}_2\text{Cl}_2$  was added, sequentially, 1.21 g (12 mmol) of triethylamine, 1.0 g (7.7 mmol) of 5,5-dimethyl-1-hexanol, and 0.97 g (8.5 mmol) of methanesulfonyl chloride. The mixture was stirred for 2 h at –10 °C, and then quenched by addition of 10 mL of ice water. Separation of the organic layer, followed by washing (10 mL of 1 M  $\text{HCl}$ , 10 mL of saturated  $\text{NaHCO}_3$ , and 10 mL of brine), drying (anhydrous  $\text{MgSO}_4$ ), concentration under reduced pressure, and purification by column chromatography (silica,  $\text{CH}_2\text{Cl}_2$ ), afforded 1.38 g (86%) of 5,5-dimethylhexyl-1-methanesulfonate as a colorless oil having  $^1\text{H}$  NMR ( $\text{CDCl}_3$ )  $\delta$  0.85 (s, 9 H), 1.15–1.20 (m, 2 H), 1.32–1.35 (m, 2 H), 1.68–1.72 (m, 2 H), 2.99 (s, 3 H), 4.21 (t, 2 H). HRMS for  $(\text{C}_9\text{H}_{21}\text{O}_3\text{S})^+$ : calcd, 209.1211; found, 209.1207.

**37,38,39,40,41,42-Hexakis(5,5-dimethyl-1-hexyloxy)-calix[6]arene (1a).** To a solution of 0.50 g (0.785 mmol) of 37,38,39,40,41,42-hexahydroxycalix[6]arene in 20 mL of anhydrous DMF was added 0.47 g (11.78 mmol) of 60%  $\text{NaH}$  in mineral oil. After the mixture was stirred for 30 min at 60 °C under a nitrogen atmosphere, 1.18 g (5.65 mmol) of 5,5-dimethylhexyl-1-methanesulfonate was then added. After additional stirring for 24 h, 30 mL of water was added, and the product mixture was allowed to cool to room temperature. The resulting precipitate was filtered and washed with water and methanol to give a yellow powder. Precipitation from  $\text{CHCl}_3/\text{CH}_3\text{OH}$  gave 0.50 g (48%) of 37,38,39,40,41,42-hexakis(5,5-dimethyl-1-hexyloxy)calix[6]arene as a white powder. Recrystallization from  $\text{CHCl}_3/\text{CH}_3\text{OH}$  (1/1, v/v) afforded 0.26 g of crystalline material (needles) having mp 235–237 °C;  $^1\text{H}$  NMR ( $\text{CDCl}_3$ )  $\delta$  0.88 (s, 54 H), 1.14–1.35 (br m, 36 H), 3.24 (br s, 12 H), 3.92 (br s, 12 H), 6.70–6.74 (m, 6 H), 6.90 (br s, 12 H). Anal. Calcd for  $\text{C}_{90}\text{H}_{132}\text{O}_6$ : C, 82.52; H, 10.15. Found: C, 82.59; H, 10.30.

**5,11,17,23,29,35-Hexabromo-37,38,39,40,41,42-hexakis(5,5-dimethyl-1-hexyloxy)calix[6]arene (2a).** A solution of 0.50 g (0.381 mmol) of 37,38,39,40,41,42-hexakis(5,5-dimethyl-1-hexyloxy)calix[6]arene and 1.02 g (5.72 mmol) of *N*-bromosuccinimide in 20 mL of 2-butanone was stirred at room temperature with access toward light for 40 h. To this solution was added 50 mL of a 10% aqueous solution of  $\text{NaHSO}_3$  (w/w), and the resulting mixture then stirred for 30 min at room temperature. The organic components were extracted with  $\text{CH}_2\text{Cl}_2$  ( $3 \times 30 \text{ mL}$ ), and the combined extract was washed with water ( $2 \times 20 \text{ mL}$ ) and dried (anhydrous  $\text{MgSO}_4$ ). Removal of solvent

(13) A preliminary account of this work has previously appeared: Lee, W.; Hendel, R. A.; Dedek, P.; Janout, V.; Regen, S. L. *J. Am. Chem. Soc.* **1995**, *117*, 6793.

(14) Markowitz, M. A.; Janout, V.; Castner, D. G.; Regen, S. L. *J. Am. Chem. Soc.* **1989**, *111*, 8192.

(15) Lee, H. S.; Isagawa, K.; Toyoda, H.; Otsuji, Y. *Chem. Lett.* **1984**, 673.

under reduced pressure afforded an oily crude product, which was triturated with hot isopropyl alcohol to give 0.38 g (56%) of 5,11,17,23,29,35-hexabromo-37,38,39,40,41,42-hexakis(5,5-dimethyl-1-hexyloxy)calix[6]arene as a colorless powder. Recrystallization from CHCl<sub>3</sub>/CH<sub>3</sub>OH (1/1, v/v) yielded 0.28 g of crystalline product having mp 264–267 °C; <sup>1</sup>H NMR (CDCl<sub>3</sub>, 60 °C) δ 0.87 (s, 54 H), 1.21–1.40 (br m, 24 H), 1.69 (br s, 12 H), 3.71–3.75 (m, 12 H), 3.88 (br s, 12 H), 6.88 (br s, 12 H). Anal. Calcd for C<sub>90</sub>H<sub>126</sub>O<sub>6</sub>Br<sub>6</sub>: C, 60.61; H, 7.12; Br, 26.88. Found: C, 60.77; H, 7.09; Br, 27.14.

**5,11,17,23,29,35-Hexacyano-37,38,39,40,41,42-hexakis(5,5-dimethyl-1-hexyloxy)calix[6]arene (3a).** A solution of 0.37 g (0.207 mmol) of 5,11,17,23,29,35-hexabromo-37,38,39,40,41,42-hexakis(5,5-dimethyl-1-hexyloxy)calix[6]arene and 1.11 g (12.40 mmol) of CuCN in 15 mL of anhydrous 1-methyl-2-pyrrolidinone was refluxed with stirring under a nitrogen atmosphere for 4 h. The temperature of the mixture was then cooled to 100 °C, and a solution made from 3.35 g (12.4 mmol) of FeCl<sub>3</sub>·6H<sub>2</sub>O plus 10 mL of concentrated HCl and 50 mL of water was then added. The mixture was stirred at 100 °C for 20 min, followed by additional stirring at room temperature for 16 h. The resulting precipitate was filtered and washed, sequentially, with 1 M HCl (20 mL), water (20 mL), and 5 mL of CH<sub>3</sub>OH to give 0.36 g of crude product. Purification by column chromatography (silica, hexane/CHCl<sub>3</sub>/acetone, 20/20/1, v/v/v) afforded 201 mg (66%) of 5,11,17,23,29,35-hexacyano-37,38,39,40,41,42-hexakis(5,5-dimethyl-1-hexyloxy)calix[6]arene as a white powder. Recrystallization from CHCl<sub>3</sub>/CH<sub>3</sub>OH (1/1, v/v) gave 36 mg of crystalline product having mp 250–251 °C; <sup>1</sup>H NMR (CDCl<sub>3</sub>) δ 0.77–0.86 (m, 54 H), 1.05–1.86 (m, 36 H), 3.58–4.22 (m, 24 H), 6.15–7.58 (m, 12 H). Anal. Calcd for C<sub>96</sub>H<sub>126</sub>N<sub>6</sub>O<sub>6</sub>: C, 78.97; H, 8.69; N, 5.76. Found: C, 78.92; H, 8.65; N, 5.75.

**5,11,17,23,29,35-Hexaamidoxime-37,38,39,40,41,42-hexakis(5,5-dimethyl-1-hexyloxy)calix[6]arene (I).** A solution of 0.146 g (0.100 mmol) of 5,11,17,23,29,35-hexacyano-37,38,39,40,41,42-hexakis(5,5-dimethyl-1-hexyloxy)calix[6]arene, 0.42 g (6.0 mmol) of hydroxylamine hydrochloride, and 0.24 g (6.0 mmol) of sodium hydroxide in a mixture of 2 mL of water, 10 mL of *tert*-butyl alcohol, and 75 mL of ethanol was stirred at 70 °C for 2 days. After being cooled to room temperature, the mixture was concentrated under reduced pressure and water (5 mL) was then added. The resulting mixture was extracted with CHCl<sub>3</sub> to give a turbid solution. Concentration under reduced pressure and purification by preparative TLC (*R*<sub>f</sub> = 0.56; silica, CHCl<sub>3</sub>/CH<sub>3</sub>OH/H<sub>2</sub>O, 65/25/4, v/v/v) afforded 43 mg (24%) of 5,11,17,23,29,35-hexaamidoxime-37,38,39,40,41,42-hexakis(5,5-dimethyl-1-hexyloxy)calix[6]arene as a colorless powder having mp >250 °C; <sup>1</sup>H NMR (DMSO-*d*<sub>6</sub>) δ 0.73–0.89 (m, 54 H), 1.22–1.31 (m, 12 H), 1.44 (br s, 12 H), 1.84 (br s, 12 H), 3.47 (d, 6 H), 3.78 (br s, 12 H), 4.46 (d, 6 H), 5.36–5.66 (m, 12 H), 6.99–7.80 (m, 12 H), 9.38–9.54 (m, 6 H). HRMS for (C<sub>96</sub>H<sub>145</sub>O<sub>12</sub>N<sub>12</sub>)<sup>+</sup>: calcd, 1658.1105; found, 1658.1093.

**5,11,17,23,29,35-Hexabromo-37,38,39,40,41,42-hexakis(1-octyloxy)calix[6]arene (2b).** By using procedures similar to those described for the preparation of 2a, a 56% yield of 2b was obtained (starting with 1b) having mp 218–219 °C; <sup>1</sup>H NMR (CDCl<sub>3</sub>, 60 °C) δ 0.95 (t, 18 H), 1.25–1.60 (m, 72 H), 3.55 (s, 12 H), 3.85 (s, 12 H), 6.95 (s, 12 H). Anal. Calcd for C<sub>90</sub>H<sub>126</sub>O<sub>6</sub>Br<sub>6</sub>: C, 60.61; H, 7.12; Br, 26.88. Found: C, 60.36; H, 6.95; Br, 27.07.

**5,11,17,23,29,35-Hexacyano-37,38,39,40,41,42-hexakis(1-octyloxy)calix[6]arene (3b).** By using procedures similar to those described for the preparation of 3a, a 18% yield of 3b was obtained (starting with 2b) having mp 213–214 °C; <sup>1</sup>H NMR (CDCl<sub>3</sub>) δ 0.85 (t, 18 H), 1.15 (m, 72 H), 3.55–4.40 (m, 24 H), 6.15–7.15 (m, 12 H). Anal. Calcd for C<sub>96</sub>H<sub>126</sub>O<sub>6</sub>N<sub>6</sub>: C, 78.97; H, 8.70; N, 5.76. Found: N, 5.65.

**5,11,17,23,29,35-Hexaamidoxime-37,38,39,40,41,42-hexakis(1-octyloxy)calix[6]arene (II).** By using procedures similar to those described for the preparation of I, a 56% yield of II was obtained (starting with 3b) having mp 259–260 °C; <sup>1</sup>H NMR (DMSO-*d*<sub>6</sub>, 60 °C) δ 0.85 (t, 18 H), 1.28 (br s, 60 H), 1.82 (br s, 12 H), 3.46 (d, 6 H), 3.75 (br s, 12 H), 4.46 (d, 6 H), 5.30–5.77 (br s, 12 H), 6.85–7.81 (m, 12 H), 9.62 (br s, 6 H). HRMS for (C<sub>96</sub>H<sub>145</sub>O<sub>12</sub>N<sub>12</sub>)<sup>+</sup>: calcd, 1658.1105; found, 1658.1102.

**37,38,39,40,41,42-Hexakis(1-dodecyloxy)calix[6]arene (1c).** By using procedures similar to those described for the preparation of 1a,

direct alkylation of 37,38,39,40,41,42-hexahydroxycalix[6]arene with 1-bromododecane afforded a 69% yield of 1c having mp 76–77 °C; <sup>1</sup>H NMR (CDCl<sub>3</sub>, 60 °C) δ 0.88 (t, 18 H), 1.28–1.41 (m, 120 H), 3.29 (s, 12 H), 3.91 (s, 12 H), 6.72 (t, 6 H), 6.92 (d, 12 H). Anal. Calcd for C<sub>114</sub>H<sub>180</sub>O<sub>6</sub>: C, 83.16; H, 11.01. Found: C, 81.11; H, 11.02.

**5,11,17,23,29,35-Hexabromo-37,38,39,40,41,42-hexakis(1-dodecyloxy)calix[6]arene (2c).** By using procedures similar to those described for the preparation of 2a, a 58% yield of 2c was obtained (starting with 1c) having mp 181–183 °C; <sup>1</sup>H NMR (CDCl<sub>3</sub>, 60 °C) δ 0.87 (t, 18 H), 1.26 (s, 108 H), 1.63 (br s, 12 H), 3.64 (br s, 12 H), 3.87 (br s, 12 H), 6.95 (br s, 12 H). Anal. Calcd for C<sub>114</sub>H<sub>174</sub>O<sub>6</sub>Br<sub>6</sub>: C, 64.59; H, 8.27; Br, 22.61. Found: C, 64.31; H, 8.23; Br, 22.46.

**5,11,17,23,29,35-Hexacyano-37,38,39,40,41,42-hexakis(1-dodecyloxy)calix[6]arene (3c).** By using procedures similar to those described for the preparation of 3a, a 36% yield of 3c was obtained (starting with 2c) having mp 198–199 °C; <sup>1</sup>H NMR (CDCl<sub>3</sub>) δ 0.82 (m, 54 H), 1.15–1.85 (m, 120 H), 3.58–4.20 (m, 24 H), 6.12–7.57 (m, 12 H). Anal. Calcd for C<sub>120</sub>H<sub>174</sub>O<sub>6</sub>N<sub>6</sub>: C, 80.22; H, 9.76; N, 4.68. Found: C, 80.26; H, 9.80; N, 4.72.

**5,11,17,23,29,35-Hexaamidoxime-37,38,39,40,41,42-hexakis(1-dodecyloxy)calix[6]arene (III).** By using procedures similar to those described for the preparation of II, a 22% yield of III was obtained (starting with 3c) having mp >233 °C; <sup>1</sup>H NMR (DMSO-*d*<sub>6</sub>, 60 °C) δ 0.84 (s, 18 H), 1.24 (br s, 108 H), 1.75 (br s, 12 H), 3.49 (t, 6 H), 3.72 (br s, 12 H), 4.48 (d, 6 H), 5.09–5.43 (m, 12 H), 6.88–7.67 (m, 24 H), 9.31 (s, 6 H). Anal. Calcd for C<sub>120</sub>H<sub>192</sub>O<sub>12</sub>N<sub>12</sub>: C, 72.25; H, 9.70; N, 8.43. Found: C, 72.36; H, 9.61; N, 6.93.

**37,38,39,40,41,42-Hexakis(1-hexadecyloxy)calix[6]arene (1d).** By using procedures similar to those described for the preparation of 1a, direct alkylation of 37,38,39,40,41,42-hexahydroxycalix[6]arene with 1-bromohexadecane afforded a 71% yield of 1d having mp 88–89 °C; <sup>1</sup>H NMR (CDCl<sub>3</sub>, 60 °C) δ 0.88 (t, 18 H), 1.27–1.41 (m, 168 H), 3.29 (br s, 12 H), 3.91 (s, 12 H), 6.72 (t, 6 H), 6.92 (d, 12 H). Anal. Calcd for C<sub>138</sub>H<sub>228</sub>O<sub>6</sub>: C, 83.58; H, 11.58. Found: C, 83.44; H, 11.41.

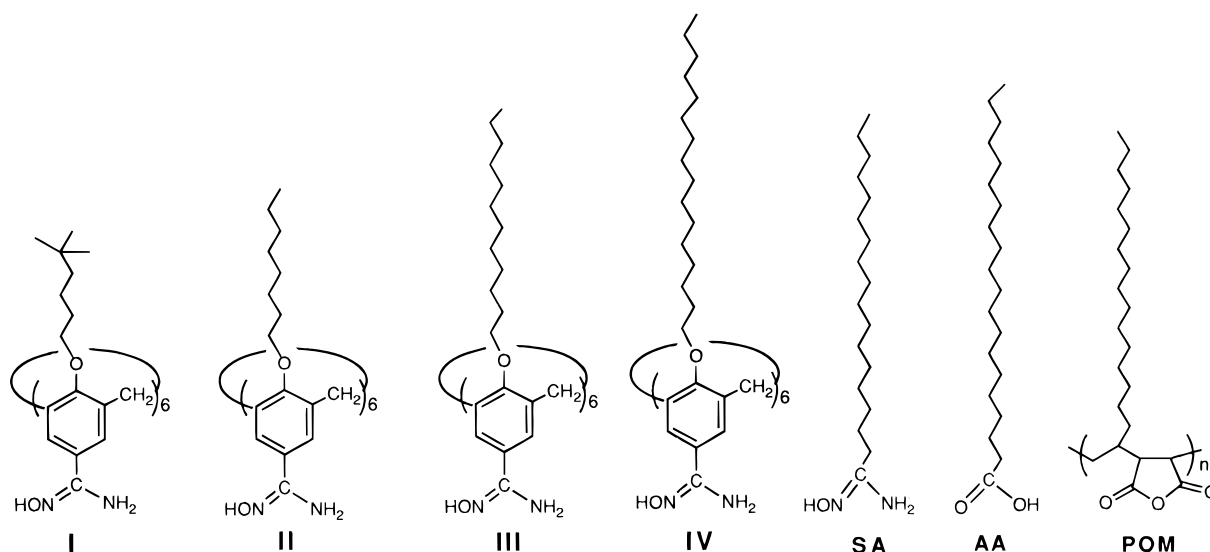
**5,11,17,23,29,35-Hexabromo-37,38,39,40,41,42-hexakis(1-hexadecyloxy)calix[6]arene (2d).** By using procedures similar to those described for the preparation of 2a, a 43% yield of 2d was obtained (starting with 1d) having mp 155–156 °C; <sup>1</sup>H NMR (CDCl<sub>3</sub>, 60 °C) δ 0.88 (t, 18 H), 1.26–1.42 (m, 156 H), 1.62 (br s, 12 H), 3.63 (br s, 12 H), 3.86 (br s, 12 H), 6.95 (br s, 12 H). Anal. Calcd for C<sub>138</sub>H<sub>222</sub>O<sub>6</sub>Br<sub>6</sub>: C, 67.47; H, 9.10; Br, 19.52. Found: C, 67.35; H, 8.90; Br, 19.64.

**5,11,17,23,29,35-Hexacyano-37,38,39,40,41,42-hexakis(1-hexadecyloxy)calix[6]arene (3d).** By using procedures similar to those described for the preparation of 3a, a 51% yield of 3d was obtained (starting with 2d) having mp 162–165 °C; <sup>1</sup>H NMR (CDCl<sub>3</sub>) δ 0.85 (t, 18 H), 1.15–1.84 (m, 168 H), 3.55–4.20 (m, 24 H), 6.12–7.57 (m, 12 H). Anal. Calcd for C<sub>144</sub>H<sub>222</sub>O<sub>6</sub>N<sub>6</sub>: C, 81.08; H, 10.48; N, 3.94. Found: C, 80.89; H, 10.70; N, 3.71.

**5,11,17,23,29,35-Hexaamidoxime-37,38,39,40,41,42-hexakis(1-hexadecyloxy)calix[6]arene (IV).** One hundred and fifty milligrams of a solution (0.42 mmol of nitrile units, 0.07 mmol calix[6]arene) and 0.09 g (2.25 mmol) of sodium hydroxide, in a mixture of 30 mL of *tert*-butyl alcohol and 90 mL of ethanol, was stirred at 70 °C for 1 week. After being cooled to room temperature, the solvent was then removed under reduced pressure. Water (30 mL) was then added to the mixture, followed by extraction with CHCl<sub>3</sub> (3 × 10 mL). The combined CHCl<sub>3</sub> extract appeared as a turbid solution. Removal of solvent under reduced pressure, followed by recrystallization (four times) from CHCl<sub>3</sub>/CH<sub>3</sub>OH/H<sub>2</sub>O (100/25/2, v/v/v), afforded 50 mg of fine white needles having *R*<sub>f</sub> = 0.6 (silica, CHCl<sub>3</sub>/CH<sub>3</sub>OH/H<sub>2</sub>O, 65/25/3, v/v/v); mp >300 °C; <sup>1</sup>H NMR (DMSO-*d*<sub>6</sub>, 80 °C) δ 0.85 (t, 18 H), 1.25 (s, 156 H), 1.72 (br s, 12 H), 3.46 (d, 6 H), 3.70 (br s, 12 H), 4.48 (d, 6 H), 5.05–5.30 (m, 12 H), 7.03–7.45 (m, 24 H), 9.21 (br s, 6 H). Anal. Calcd for C<sub>144</sub>H<sub>240</sub>O<sub>12</sub>N<sub>12</sub>: C, 74.12; H, 10.30; N, 7.21. Found: C, 74.19; H, 10.30; N, 6.92.

**Stearoamidoxime (SA).** A solution composed of stearonitrile (357 mg, 1.35 mmol), hydroxylamine (468 mg, 6.63 mmol), sodium hydroxide (269 mg, 6.73 mmol), water (4 mL), *tert*-butyl alcohol (20 mL), and ethanol (150 mL) was stirred at 70 °C for 48 h. After being cooled to room temperature, the solution was concentrated under reduced pressure and extracted with 3 × 10 mL of acetone. Subsequent

Chart 1



concentration under reduced pressure and purification by preparative thin layer chromatography [silica,  $\text{CHCl}_3/\text{CH}_3\text{OH}$  (10/1),  $R_f = 0.41$ ] and recrystallization from ethanol afforded 117 mg (29%) of stearoamidoxime as a white solid having mp 75–77 °C;  $^1\text{H NMR}$  (acetone- $d_6$ , 40 °C)  $\delta$  0.88 (t, 3 H), 1.30 (m, 30 H), 1.55 (m, 2 H), 2.02 (t, 2 H), 4.87 (br s, 2 H), 7.80 (br s, 1 H). HRMS for  $(\text{C}_{18}\text{H}_{38}\text{ON}_2)^+$ : calcd, 299.3062; found, 299.3067.

**Surface Pressure–Area Isotherms.** Surface pressure–area isotherms were recorded by use of an MGW Lauda film balance, which was equipped with a computerized data acquisition station. All isotherms were measured at 25 °C. Water (ca. 1 L), which was used as a subphase, was purified *via* a Milli-Q filtration system and purged with nitrogen for 15 min. Before addition to the film balance, the surface of this degassed water was removed *via* aspiration in order to remove surface-active contaminants. All surfactant solutions were spread onto the aqueous subphase having a surface area of 600  $\text{cm}^2$ , using a gas-tight, 50  $\mu\text{L}$  Hamilton syringe. Solutions of **I**, **II**, and **III** were made by using a mixed solvent [ $\text{CHCl}_3/\text{CH}_3\text{OH}$ , 8/3 (v/v)]; typical concentrations that were used were ca. 1.2 mg/mL. A spreading solution of **SA** (1.2 mg/mL) was made by using  $\text{CHCl}_3/\text{CH}_3\text{OH}$  (2/3, v/v) as solvent; with **IV**, a solution (0.17 mg/mL) made from  $\text{CHCl}_3/\text{CH}_3\text{OH}$  (5/1, v/v) was used. **POM** and **AA** were spread as a chloroform solution, using a concentration of 1.0 mg/mL. Actual concentrations were determined by direct weighing of aliquots after evaporation of solvent with a Cahn 27 electrobalance. In all cases, spreading solvents were allowed to evaporate for at least 30 min prior to compression under a flow of nitrogen. Limiting areas were determined by extrapolating from the condensed region to zero surface pressure.

**Surface Viscosity Measurements.** For surface viscosity experiments, a home-built canal viscometer (192 mm  $\times$  40 mm solid Teflon block, having a centrally located 6.5 mm slit) was placed in front of the compressing barrier and the monolayer was compressed at a rate of 25  $\text{cm}^2/\text{min}$ . When the surface pressure began to rise, the compression speed was decreased to 13  $\text{cm}^2/\text{min}$  to allow for more precise control over the surface pressure. Compressions were stopped when a target pressure of 20 dyn/cm was reached. The resulting monolayer was then allowed to equilibrate at this pressure for 3 h. After this period of time, the moving barrier was expanded at the maximum speed of 120  $\text{cm}^2/\text{min}$ , leaving the canal viscometer at its original position. The resulting surface pressure was then recorded as a function of time. The rate of surface pressure decrease was taken as a measure of the surface viscosity of the monolayer.

**Supports.** Supports that were made from PTMSP were prepared by using a casting technique. All of the PTMSP that was used in this work was generously supplied to us by Air Products and Chemicals, Inc. (Allentown, PA), having  $\text{MW} = 8 \times 10^5$  (intrinsic viscosity method). A typical casting apparatus consisted of a Pyrex glass square (8 in.  $\times$  8 in.  $\times$  1/8 in.), an aluminum centering ring seal, 160 ISO

flange size (Kurt J. Lesker Co., Allentown, PA), and five (2.10 in. o.d.  $\times$  1.64 in. i.d.  $\times$  0.010 in.) low carbon steel washers (Boker's, Inc., Allentown, PA). The Pyrex glass square, ring seal, and five washers were cleaned with chloroform, methanol, and acetone, with the aid of kimwipes. The ring seal was then adhered to the glass square by using a 5% toluene solution (HPLC grade) of PTMSP, which acted as a "glue". The steel washers were placed symmetrically within the ring seal/glass square casting unit. A PTMSP/toluene casting solution (ca. 180 mg/30 mL) was then poured into the ring seal and covered with a large piece of filter paper (Whatman qualitative circles, 18.5 cm) in order to keep the casting unit dust-free. The toluene was allowed to evaporate for at least 15 h, leaving a PTMSP film across the steel washers and glass square. A surgical blade (S/P Surgical Blades, Baxter Diagnostics) was used to cut out the individual washers. Water was poured into the ring seal to help separate the washers. The PTMSP cast films were placed between several large pieces of filter paper and allowed to dry for at least 24 h. The resulting membranes, having a typical thickness of ca. 15  $\mu\text{m}$ , were placed in antistatic bags for at least 15 min prior to use in composite membrane fabrication.

**Fabrication of Composite Membranes.** PTMSP/surfactant composite membranes were prepared by conventional vertical Langmuir–Blodgett (LB) "dipping" with use of an MGW Lauda film balance. All transfers were performed in a positive pressure clean room. The subphase for each experiment was pure water, which was maintained at 25 °C. When  $\text{CdCl}_2$  was used, 0.5 mM solutions were prepared from 99.99% salt (Aldrich). Spreading solvents (see Surface Pressure–Area Isotherms section for details) were allowed to evaporate for at least 30 min prior to compression. A nitrogen flow of ca. 175  $\text{cm}^3/\text{min}$  at the gas-subphase interface was maintained throughout each experiment. The dipping speed that was used for each monolayer transfer was 4 mm/min. Monolayers of **I**, **II**, **III**, and **SA** were transferred at a constant pressure of 40 dyn/cm after a single compression. Monolayers of **POM** and **AA** were transferred with a constant surface pressure of 30 dyn/cm after a single compression. Drying of the LB films between bilayers of **I**, **II**, and **III** was carried out above the air–water interface under a flow of nitrogen for at least 60 min; for bilayers that were made from **SA**, **AA**,  $\text{AA}/\text{Cd}^{2+}$ , and **POM**, a delay (drying) time of 30 min was used. Transfer ratios of **I**, **II**, and **III** onto PTMSP cast films were typically 1.0 and 1.2 for down- and up-trips, respectively. Transfer ratios for **SA** onto PTMSP cast films were typically 0.9 and 1.1 for down- and up-trips; for **POM**, the typical transfer ratios were 1.0 and 1.2 for the down- and up-trips. Transfer ratios for **AA** on PTMSP were 1.2 and 0.7 for down- and up-trips, respectively; for **AA** that was spread over a 0.5 mM  $\text{CdCl}_2$  solution, transfer ratios were typically 1.2 and 1.2 for down- and up-trips, respectively. Monolayers of **IV** were transferred at a constant surface pressure of 30 dyn/cm after three compressions and two expansions. Drying between bilayers of **IV** was carried out under ambient conditions (23 °C, 22 h, away from the air/water interface). Transfer ratios of **IV**

onto PTMSP were typically 0.95 and 1.2 for initial down- and up-trips, and 1.0 and 1.2 for subsequent down- and up-trips. All composite membranes were carefully placed in tin specimen boxes (Fisher Scientific) which were lined with Whatman 5.5 cm qualitative filter papers (LB film side up). Each composite membrane was allowed to remain in the laboratory ambient (clean room) for a minimum of 12 h before gas permeation measurements were carried out. For prolonged storage, the PTMSP/LB composite membranes were placed in a desiccator that contained anhydrous CaSO<sub>4</sub>, which was maintained under an argon atmosphere.

**Gas Permeation Measurements.** Gas permeation measurements were made with a home-built stainless steel permeation apparatus (Figure 4). The gases studied were He (Airco, grade 4.7) and N<sub>2</sub> (JWS Technologies, prepurified grade). A membrane to be measured was placed in the permeation cell between two Viton rubber O-rings (3.45 cm i.d., Scientific Instrument Services, Inc.) with a support screen (4.70 cm, Millipore Corp.) and held securely with a quick flange clamp (Scientific Instrument Services, Inc., not shown). Polymer/surfactant composites were always placed in the cell such that the LB film faced the high pressure side of the pressure gradient. The permeant gas travelled from the gas cylinder to an inline filter (15 μm) and elastomer diaphragm regulator (Brooks Instrument, 8601D), which was connected to a Heise gauge port. Another plastic tubing line connected from the Heise gauge outlet to the permeation cell. The pressure gradient that was applied to each membrane was 0.7 atm (10 psig). After passing through the membrane, the gaseous permeant was directed into a 40 cm long glass U-tube flowmeter (2 mm i.d.). The volumetric flow rate of the gas was then measured by recording the time ( $t_f - t_i$ ) that was required for a methyl isobutyl ketone solution containing crystal violet to travel a set distance ( $d_f - d_i$ ), thereby sweeping out a defined volume. Measurements were taken until steady-state values were achieved (typically 1 to 2 h). At least ten volumetric flow rates were recorded for each membrane, and the mean and standard deviations were determined. The normalized flux was calculated with use of the mean volumetric flow rate, the area that was available for flow (9.36 cm<sup>2</sup>), and the pressure gradient (0.7 atm) that was employed. This procedure was repeated for the next permeant gas. Selectivity ratios were simply the ratio of the normalized fluxes for He and N<sub>2</sub> (see eqs 1 and 2). In general, the permeation properties were first measured for He and then for N<sub>2</sub>.

**X-ray Photoelectron Spectroscopy.** Surface analyses of bare PTMSP, PTMSP/I, and PTMSP/SA composites were performed with a Scienta ESCA-300 spectrometer (Scienta Instruments AB, Uppsala, Sweden). Composite membranes consisted of four LB monolayers that were deposited onto ca. 20 μm thick PTMSP films, which were coated onto silicon wafers (ca. 2 cm<sup>2</sup>). Transfer ratios were typically 1.0 ± 0.2 for each down- and up-trip. The ESCA-300 spectrometer was equipped with an X-ray source, a monochromator, an imaging lens, a hemispherical analyzer, and a multichannel detector. The X-ray source was a rotating titanium alloy anode. An electron beam directed on the aluminum band of the anode produced Al Kα radiation, which was monochromized with seven toroidally bent α-quartz crystals. The X-rays were focused on the composite membrane surface at 45° from the analyzer. Photoelectrons from the composite were collected by a multielement lens and focused on a slit aperture pair at the entrance plane of a hemispherical (radius = 30 cm) electron energy analyzer (HMA). The multichannel detector, placed at the exit of the HMA, consisted of two microchannel plates, a P10 phosphor, and a CCD TV camera. Analysis was carried out at a pressure range of 10<sup>-9</sup> to 10<sup>-10</sup> Torr; degassing typically required ca. 30 min. A take-off angle of 15° was used for each experiment. The XPS analysis focused on C, Si, N, and O that were present on the surface of the composite.

**Transmission FTIR Spectroscopy.** Analyses of bare PTMSP cast film and PTMSP/SA composites were made with a Mattson Polaris FTIR spectrometer, equipped with WinFirst Fourier software tools for Microsoft systems. A freshly prepared PTMSP cast film was first analyzed (1200 scans) under a nitrogen atmosphere. Four monolayers of SA were then deposited onto this PTMSP surface with the LB vertical dipping method; transfer ratios were 1.0 ± 0.2. After allowing the composite to air-dry for 24 h in the clean room, additional FTIR spectra (1200 scans) were recorded. Several different regions of the composite

were measured to obtain a clear SA spectrum after subtracting the bare PTMSP spectrum as a "background".

## Results

**Surfactant Design and Synthesis.** Specific calix[6]arenes that were chosen as synthetic targets for the present study were **I**, **II**, **III**, and **IV**. The amide oxime moiety was viewed as an attractive head group based on its strong hydrophilicity and its potential for monolayer stabilization via intermolecular hydrogen bonding. Calix[6]arenes **I** and **II**, which are structural isomers, differ only in the bulkiness of their alkyl chains and their potential for closing off their "molecular pores". Examination of **I** by CPK space-filling models indicates that the bulky *tert*-butyl groups should prevent closure of its molecular pore, when held in a cylindrical conformation such that all of the amide oxime groups define one face of the molecule; with **II**, however, closure of these pores by having the alkyl chains fold into the void of the calix[6]arene is a distinct possibility. The key issue, here, is whether attractive van der Waals forces among the alkyl chains are maximized through intramolecular or intermolecular interactions in the monolayer state. If intramolecular forces were dominant, then pore closure should be favored; if intermolecular forces were more important, however, then the pores should remain open. Since van der Waals forces decrease with hydrocarbon branching, one might expect to observe a more cohesive monolayer with **II** if intermolecular interactions were dominant. In order to probe this question further, calix[6]arenes **III** and **IV** were chosen as additional synthetic targets. Here, elongation of the alkyl chains would be expected to enhance the cohesiveness of a monolayer if intermolecular forces were of major importance.

To place the barrier properties of these calix[6]arene assemblies into perspective, the permeation properties of analogous composites that were prepared from conventional single chain surfactants [i.e., multilayers of arachidic acid (**AA**), cadmium arachidate (**AA**/Cd<sup>2+</sup>), and a single chain surfactant bearing an amide oxime head group (stearoamideoxime, **SA**)] and a polymeric surfactant [poly(1-octadecene-*co*-maleic anhydride) (**POM**)] were defined. In principle, these single chain surfactants have the potential for "slithering" through the micropores of PTMSP and for entering its bulk phase. Such disassembly should then result in defect formation and a reduction in permeation selectivity. The polymeric surfactant (**POM**) was of interest since individual alkyl chains have the potential for penetrating the micropores of PTMSP, but the entire polymer molecule should remain at its surface. How such penetration would affect the permeation properties of the LB assembly was an additional question that we sought to answer.

The synthetic approaches that were used to prepare calix[6]arenes **I**, **II**, **III**, and **IV** are outlined in Scheme 1. In brief, alkylation of 37,38,39,40,41,42-hexahydroxycalix[6]arene with a suitable alkylating agent, followed by bromination with *N*-bromosuccinimide, cyanation, and addition of hydroxylamine, afforded the desired amphiphiles. A branched mesylate, which was required for the synthesis of **I**, was prepared by sequential tosylation of 3-buten-1-ol, coupling with *tert*-butyl cuprate, hydroxylation, and mesylation (Scheme 2). The single-chain surfactant, **SA**, was prepared by direct addition of hydroxylamine to stearonitrile.

**Monolayer Properties.** Surface pressure–area isotherms that were recorded for **I**, **II**, **III**, and **IV** over a pure water subphase at 25 °C are shown in Figure 1; corresponding isotherms for **SA**, **AA**, **AA**/Cd<sup>2+</sup>, and **POM** are presented in Figure 2. Limiting areas that were determined by extrapolation from the condensed region of each isotherm to zero surface

## Scheme 1

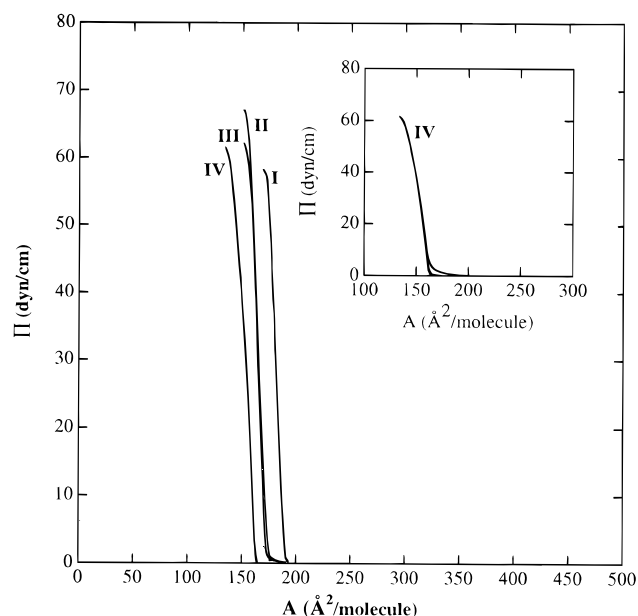
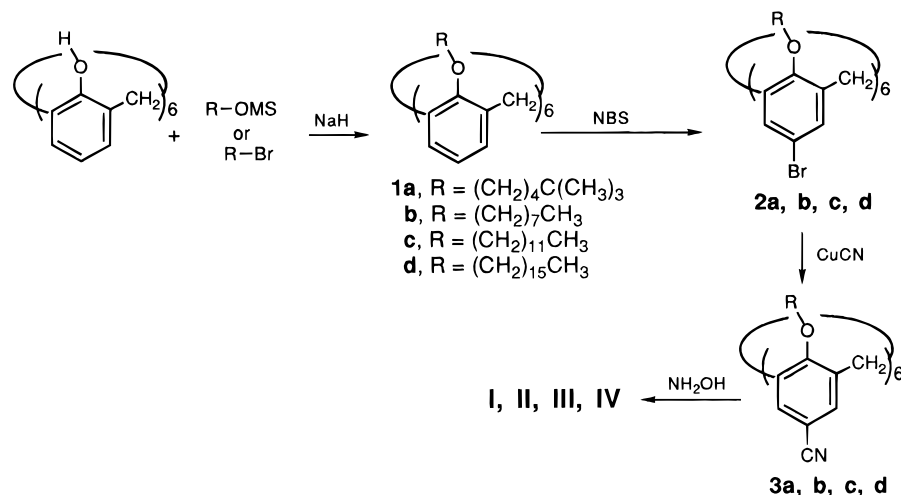
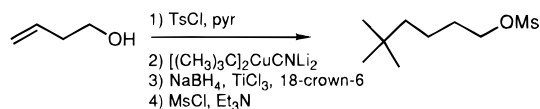


**Figure 1.** Surface pressure–area isotherms for **I**, **II**, **III**, and **IV** over a pure water subphase at 25 °C. The isotherm that is shown for **IV** represents the third compression. For **I**, **II**, and **III**, no difference between the first and third compression was observed. Inset: Isotherm for **IV**, which shows hysteresis between the first, second, and third compressions.

## Scheme 2



pressure were 190, 175, 175, and 162 Å<sup>2</sup>/molecule for **I**, **II**, **III**, and **IV**, respectively; the limiting areas for **SA**, **AA**, and **AA/Cd<sup>2+</sup>** were 19, 20 and 20 Å<sup>2</sup>/molecule, respectively. A repeat unit limiting area for **POM** was estimated to be 36 Å<sup>2</sup>. With the exception of **IV**, all of these surfactants produced monolayers with no detectable hysteresis. In the case of **IV**, stable monolayers were formed but significant hysteresis was clearly evident (Figure 1). After two consecutive compressions and expansions, however, this hysteresis was eliminated.

To judge the cohesiveness of these calix[6]arenes in the monolayer state, we examined their relative surface viscosities at the air–water interface by use of a canal viscometer (see Experimental Section). For purposes of comparison, the relative surface viscosities of monolayers that were prepared from **SA**

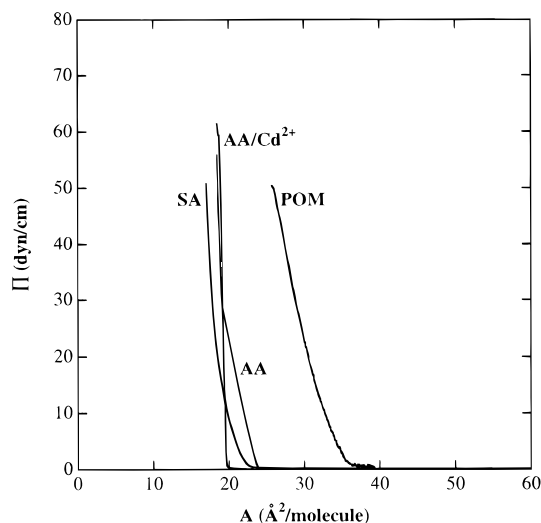


**Figure 2.** Surface pressure–area isotherms for **AA**, **SA**, and **POM** over a pure water subphase at 25 °C; the isotherm observed for **AA** spread over 0.5 mM CdCl<sub>2</sub> is also shown.

and **POM** were also examined. Qualitatively, monolayers that were formed from **I**, **SA**, and **POM** showed relatively low viscosity; in each case, there was a precipitous drop in surface pressure when the monolayer was exposed to a 6.5 mm slit (Figure 3). In contrast, monolayers that were assembled from **II** and **III** were considerably more viscous. Extraordinarily high surface viscosity was found in the case of **IV**, where only a small pressure drop (<0.5 dyn/cm) was recorded after 2 h.

**Fabrication and Permeation Properties of Composite Membranes.** By using standard LB vertical dipping methods, composite membranes were fabricated with even numbers of monolayers of surfactant and 15 μm thick cast films of PTMSP as support material. The specific protocols that were followed are described in the Experimental Section. In all cases, efficient transfers were observed during down-trips (into water) and up-trips (into air) as judged by the transfer ratios. Specifically, the decrease in monolayer area at the air–water interface divided by the geometrical surface area of the substrate that passed, vertically, through the interface was generally 1.0 on the down-trips and 1.2 for the up-trips.

The permeation properties of each composite, with respect to He and N<sub>2</sub>, were then determined by use of a home-built apparatus (Figure 4). A detailed description of this apparatus, as well as the protocols for obtaining volumetric flow rates (**F**), are given in the Experimental Section. Normalized fluxes

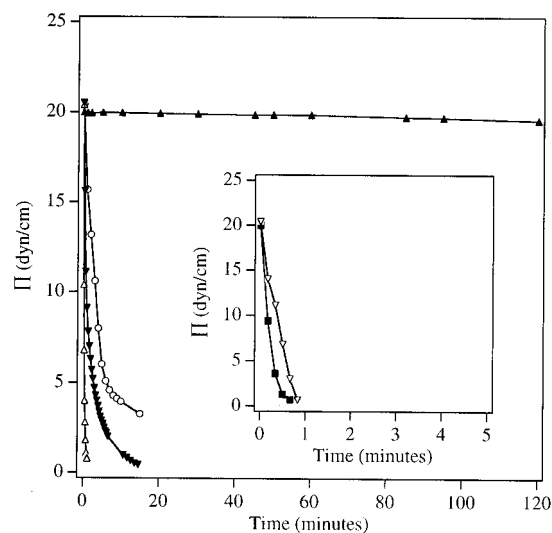


**Figure 3.** Surface pressure of monolayers formed from **I** ( $\Delta$ ), **II** ( $\circ$ ), **III** ( $\nabla$ ), and **IV** ( $\blacktriangle$ ) at 25 °C on pure water as a function of time of exposure to a 6.5 mm slit opening (canal viscometer); the initial surface pressure was 20 dyn/cm. The inset shows the results of similar experiments for **SA** ( $\blacksquare$ ) and **POM** ( $\nabla$ ).

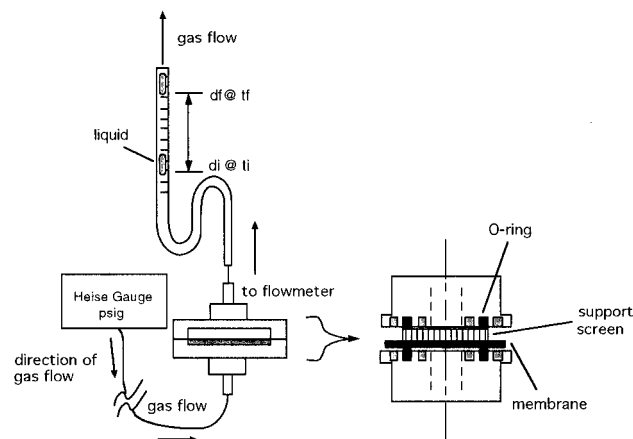


**Figure 4.** Schematic representation of the home-built permeation apparatus (not drawn to scale).

( $P/l$ ) were then calculated according to eq 1, where  $P$  represents the permeability coefficient that characterizes the composite membrane—permeant combination,  $l$  is the thickness of the composite membrane,  $A$  is the membrane's cross-sectional area, and  $\Delta p$  is the pressure gradient that was employed.<sup>16</sup> Specific normalized flux values that were measured for bare PTMSP, and for each of the composite membranes that were fabricated in this study, are listed in Tables 1 and 2.

$$\frac{P}{l} = \frac{F}{A(\Delta p)} \quad (1)$$

Deposition of up to four monolayers of **AA**, **AA/Cd<sup>2+</sup>**, and **SA** onto PTMSP did not significantly alter the barrier properties of the support; in all cases, the He and N<sub>2</sub> normalized flux values remained essentially unchanged. In contrast, deposition of two layers of **POM** resulted in a moderate decrease in the normalized flux of He and a greater decrease in the normalized flux of N<sub>2</sub>. If we define permeation selectivity,  $\alpha$ , as the normalized flux of He divided by the normalized flux of N<sub>2</sub> (eq 2), then a bilayer composite (2 monolayers of **POM** on PTMSP) showed a selectivity that was similar to what would be predicted based on Graham's law [i.e.,  $\alpha(\text{He}/\text{N}_2) = 2.6$ ]. Analogous membranes

**Table 1.** Flux of He and N<sub>2</sub> through Conventional Surfactant/PTMSP Composites<sup>a</sup>

surfactant	monolayers	$10^6 P/l$ (cm <sup>3</sup> /cm <sup>2</sup> ·s·cm Hg)		He/N <sub>2</sub> ( $\alpha$ ) (composite)
		He	N <sub>2</sub>	
none	0	530	579	0.91
	0	474	530	0.90
<b>AA</b>	4	519	592	0.88
	4	537	592	0.91
<b>AA/Cd<sup>2+</sup></b>	4	532	603	0.88
	4	528	586	0.90
<b>SA</b>	2	521	585	0.89
	4	541	592	0.91
<b>POM</b>	4	499	571	0.88
	2	452	197	2.3
	4	374	71.1	5.2
	6	288	40.0	7.2
	8	264	24.8	10.6
	10	218	17.3	12.6

**Table 2.** Flux of He and N<sub>2</sub> through Calix[6]arene/PTMSP Composites<sup>a</sup>

surfactant	monolayers	$10^6 P/l$ (cm <sup>3</sup> /cm <sup>2</sup> ·s·cm Hg)		He/N <sub>2</sub> ( $\alpha$ ) (composite)
		He	N <sub>2</sub>	
none	0	530	579	0.91
	0	474	530	0.90
<b>I</b>	2	469	113	4.1
	2	352	58.3	6.0
	4	317	12.4	26
	4	226	6.9	33
	6	264	5.8	46
	8	171	3.7	46
<b>II</b>	10	79	1.3	61
	2	350	20.0	18
	2	269	17.7	15
	4	176	4.4	40
<b>III</b>	4	167	3.6	46
	4 <sup>b</sup>	158 <sup>b</sup>	3.04 <sup>b</sup>	51.9 <sup>b</sup>
	4 <sup>c</sup>	586 <sup>c</sup>	650 <sup>c</sup>	0.9 <sup>c</sup>
	2	289	22.0	13
	2	211	17.9	12
	4	154	3.0	51
<b>IV</b>	4	136	2.5	56
	6	65.3	0.77	85
	8	56	0.76	74
	10	40.6	0.56	73
	2	235	11.3	20.7
	2	202	7.97	25.5
	4	78.3	0.46	170
	4	49.6	<0.29	>171

<sup>a</sup> Normalized flux ( $P/l$ ) equals the observed flow rate, divided by the area of the membrane (9.36 cm<sup>2</sup>) and by the pressure gradient (0.7 atm) employed. Each set of data corresponds to a separate composite membrane made by using an ca. 15  $\mu\text{m}$  thick PTMSP support plus multiple layers of amphiphile. All measurements were made at ambient temperatures. Values were obtained from 5–10 independent measurements; the error in each case was  $\pm 5\%$ . <sup>b</sup> Prior to gentle wiping of the surface with a clean tip swab. <sup>c</sup> After gentle wiping of the surface with a clean tip swab.

that were fabricated with larger numbers of monolayers, however, showed an increase in permeation selectivity.

$$\alpha = \frac{(P/l)\text{He}}{(P/l)\text{N}_2} \quad (2)$$

In sharp contrast, those composite membranes that were fabricated from each of the calix[6]arene-based LB films showed permeation selectivities that exceeded Graham's law, even when only a single bilayer of surfactant was used (Table 2). Analogous composite membranes that were fabricated with larger numbers of monolayers generally showed further increases in permeation selectivity. The most notable membranes were

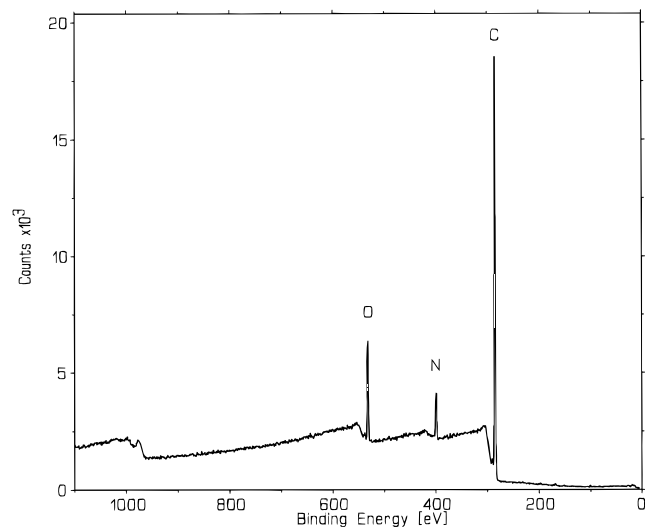


**Figure 5.** X-ray photoelectron spectrum of PTMSP/II (four monolayers).

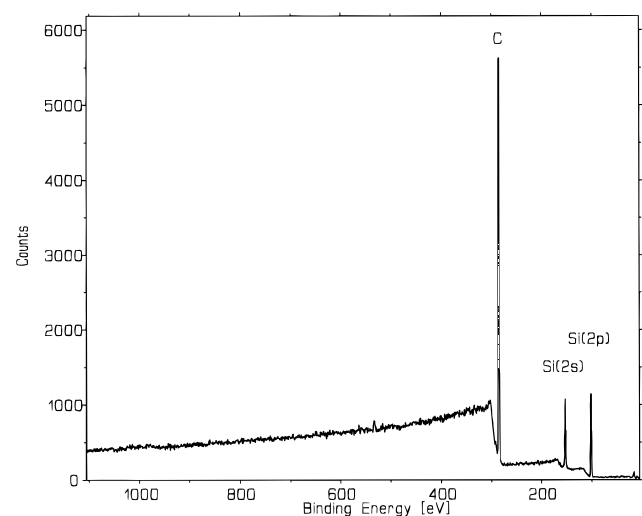


**Figure 6.** X-ray photoelectron spectrum of PTMSP/SA (four monolayers).

those that were made with four monolayers of **IV**, where the He/N<sub>2</sub> selectivity approached 200!

#### Surface Analysis by X-ray Photoelectron Spectroscopy.

To confirm the presence of **II** on the surface of PTMSP after LB deposition, a sample was analyzed by X-ray photoelectron spectroscopy (XPS). As can be seen in Figure 5, the clear presence of C, N, and O on the surface of the composite and the absence of Si provides strong evidence for an intact calix[6]arene film. Similar analysis of PTMSP/SA, however, showed no evidence of the surfactant on the polymer's surface; only the carbon and silicon atoms of the PTMSP were apparent (Figure 6). That SA was, in fact, transferred to the PTMSP support was confirmed by transmission FTIR spectroscopy. Specifically, the C–H bands of the SA at 2926 and 2855 cm<sup>-1</sup> were observed after background subtraction of the PTMSP (Figure 7).

**Robustness of Calix[6]arene/PTMSP Composites.** To judge the robustness of a calix[6]arene/PTMSP composite, a typical four-monolayered membrane was fabricated from **II** plus PTMSP and allowed to remain in a desiccator under an argon atmosphere for 4 months. Analysis of its permeation properties before and after this storage period showed no significant differences. However, gentle wiping of the surface with a clean tip swab substantially altered its permeation properties. Specif-

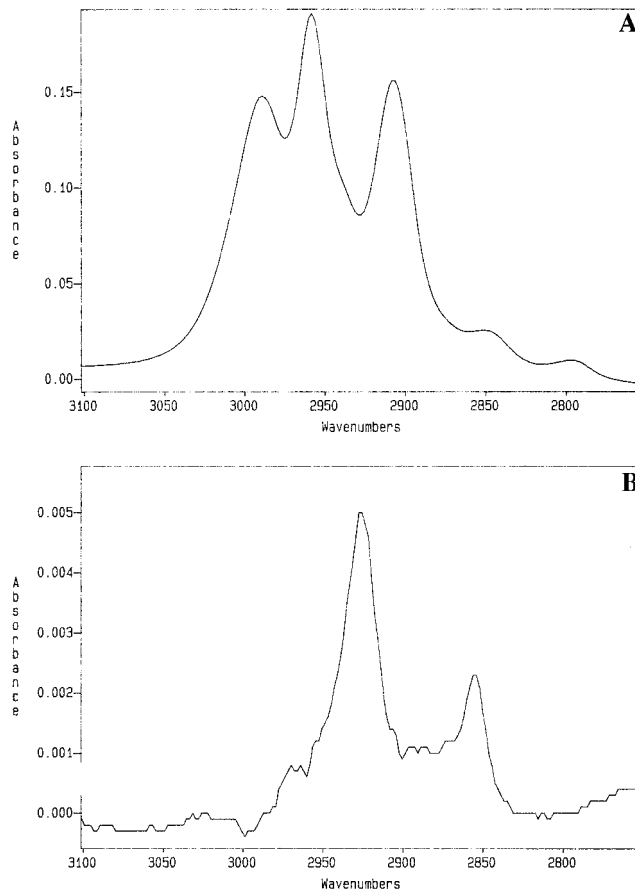


**Figure 7.** FTIR spectrum of (A) PTMSP and (B) PTMSP/SA (four monolayers) after background subtraction of PTMSP.

ically, the resulting barrier properties were almost identical with that of bare PTMSP (Table 2).

## Discussion

**Monolayer Properties.** The surface pressure–area isotherm behavior of SA, AA, AA/Cd<sup>2+</sup>, and POM was as expected. Arachidic acid showed its characteristic liquid condensed to ordered-like solid state transition at ca. 28 dyn/cm.<sup>17</sup> When compressed over a cadmium subphase, the absence of the liquid phase was clearly evident.<sup>18,19</sup> Monolayers that were formed from SA appeared to be somewhat more compressible than that of AA; in this case, no sharp phase transition was apparent. The limiting areas that were estimated for SA, AA, and AA/Cd<sup>2+</sup> are consistent with surfactant assemblies that contain a near-maximum in hydrocarbon density. In the case of POM, the maleic anhydride groups produce a more loosely packed assembly, as reflected by a limiting area of 36 Å<sup>2</sup> per repeat unit.

Examination of the surface pressure–area isotherm behavior for **I**, **II**, **III**, and **IV** reveals similar compressibility but slightly different limiting areas. If one assumes that all of the amide oxime groups are in contact with the water surface, that the calix[6]arene framework adopts a near-cylindrical conformation, and that all of the alkyl chains are extended into air, then the limiting areas that would be expected for **II**, **III**, and **IV** would be ca. 160 Å<sup>2</sup>/molecule (CPK models). Although this value is in excellent agreement with the limiting area that has been

(17) Gabrielli, G.; Gvarni, G. G. T.; Ferroni, E. *J. Colloid Interface. Sci.* **1976**, *54*, 424.

(18) Chollet, P. A. *Thin Solid Films* **1978**, *52*, 343.

(19) Rabolt, J. F.; Burns, F. C.; Schlotter, W. E. *J. Chem. Phys.* **1983**, *78*, 946.

observed for calix[6]arene **IV**, the limiting areas for **II** and **III** appear to be slightly larger. Repetitive examination of each of these surfactants (including different preparations) suggests that this difference is, in fact, real. One possible explanation for a lower limiting area for **IV** would be that stronger intermolecular hydrophobic interactions between the alkyl chains induce a more cylindrical conformation of the calix[6]arene; with **II** and **III**, a partial splay of the calix[6]arene framework could lead to larger areas. Nonetheless, the general similarity of the limiting areas of **II**, **III**, and **IV**, together with the significant differences in their alkyl chain lengths, provide a compelling “classic Langmuir” argument that these chains are extended into air.<sup>20</sup> The larger limiting area that has been observed for **I** is fully consistent with a predicted value of 190 Å<sup>2</sup>/molecule, based on CPK models. In this case, the bulky *tert*-butyl groups increase the overall cross-sectional area of the molecule.

The most notable feature among these calix[6]arene-based surfactants, with respect to their surface pressure–area isotherm behavior, is the hysteresis that has been observed with **IV**. The simplest explanation for such hysteresis, we believe, is that strong intermolecular hydrophobic interactions lead to partially separated “islands” of surfactant during the first compression. As the monolayer is then expanded and recompressed, the monolayer is mechanically forced into a more densely-packed state. Although partial retention and subsequent release of the spreading solvent could also account for this behavior, the unusually high surface viscosity that is associated with **IV** (*vide ante*) strongly suggests that this island model is more probable.

Surface viscosities that have been observed for monolayers of **II**, **III**, and **IV** support a model in which intermolecular hydrophobic interactions between neighboring alkyl chains dominate over intramolecular interactions. The relatively high viscosity that is associated with monolayers of **IV** clearly reflects a more cohesive assembly and stronger intermolecular forces. Since the only difference among **II**, **III**, and **IV** is the length of their alkyl chains, and since **IV** contains the longest chains, we conclude that intermolecular interactions between neighboring alkyl chains must be very strong. The fact that monolayers of **II** and **III** exhibit significantly greater cohesiveness at the air/water interface, compared with those of **I**, can also be accounted for in terms of stronger hydrophobic interactions; i.e., branching of the alkyl chains would be expected to reduce the magnitude of the van der Waals attractions. If intermolecular hydrogen bonding between neighboring amide oxime groups also contributes to the cohesiveness of monolayers of **II**, **III**, and **IV**, then the relatively low surface viscosity of **I** may also be due, in part, to a decrease in such bonding as a result of the greater splay of the molecule.

**Disassembly of Langmuir–Blodgett Films on PTMSP.** The permeation properties that have been observed for composites derived from **AA**, **AA**/Cd<sup>2+</sup>, and **SA** plus PTMSP are in sharp contrast to those that have been made from **I**, **II**, **III**, **IV**, and **POM**. On the basis of these permeability data alone, it would appear as if the single chain surfactants were not even present on the surface of the support. Analysis of a PTMSP/**SA** (four monolayers) composite by X-ray photoelectron spectroscopy, in fact, provides clear and direct evidence for the absence of **SA** on the surface of PTMSP. The fact that very good Y-type transfers of **SA** were observed for the down- and up-trips, however, implies that transient LB films were formed on the surface of the support. The appearance of **SA** within the film, as seen by transmission FTIR spectroscopy, together with these permeation and XPS results, constitutes strong

evidence for disassembly of the LB film and absorption of the surfactant into the bulk polymer phase.

**Assembly of Langmuir–Blodgett Films On PTMSP.** Permeation and spectroscopic results that have been obtained with **II** indicate that this surfactant is capable of forming intact LB films on the surface of PTMSP. Thus, deposition of only a single bilayer of **II** onto PTMSP affords a He/N<sub>2</sub> permeation selectivity that is ca. 5 times greater than that predicted by Graham’s law. The fact that this selectivity increases with additional bilayers of the calix[6]arene further indicates that some “sealing” within the LB film has taken place. The observation that simple wiping of such a surface with a clean tip swab converts its permeation characteristics to those of bare PTMSP provides further evidence that the assembly resides at the surface of the support. Finally, the XPS results that have been obtained for a four-monolayer composite of **II** plus PTMSP provides direct evidence for an intact calix[6]arene film on the surface of PTMSP.

Very similar permeability results have been obtained for LB films that were prepared from **I**, **III**, and **IV**. In the case of **I**, however, the relatively low selectivity that is associated with a single bilayer composite may be accounted for by a reduced cohesiveness within the assembly and a greater tendency for defect formation (*vide ante*). Deposition of additional monolayers of **I** does, however, help to “patch up” these defects. Given the strong cohesiveness of **IV** in the monolayer state, as judged by surface viscosity, the high permeation selectivity that has been found with only four monolayers is not so surprising. Presumably, this strong cohesiveness translates into a reduced tendency for defect formation and a higher percentage of permeation through the bulk of the LB film. Composite membranes that were fabricated from multilayers of the polymeric surfactant, **POM**, showed significantly lower permeation selectivities relative to those that were made from the calix[6]arenes. However, these selectivities generally exceeded that which is predicted by Graham’s law.

**On the Uniqueness and Tunability of Calix[6]arene-Based LB Films as Permeation-Selective Membranes.** Early studies from our laboratories have established the uniqueness of PTMSP as support material for calix[6]arene-based LB films in creating permeation-selective membranes. The present findings show that these calix[6]arene-based amphiphiles, when used in combination with PTMSP, are also unique relative to conventional single chain surfactants. In contrast to single chain surfactants, which are able to “slither” through the pores of PTMSP and enter the bulk phase, the calix[6]arenes are sufficiently large such that similar disassembly is prevented. It would appear, therefore, that a key factor in creating permeation-selective LB films is to use *individual surfactants that can span individual holes on the surface of the support*. Thus, a strategy that relies upon strong intermolecular forces between large numbers of surfactants to “bridge the gaps” of the support is unlikely to be successful. The ability of **POM** to produce permeation-selective LB films on PTMSP is consistent with this view. Here, a single **POM** molecule that can cover a micropore of PTMSP is capable of producing selectivities that exceed Graham’s law. Whether or not other polymeric surfactants can achieve the level of permeation selectivity that is associated with these calix[6]arenes remains to be determined.

Comparison of the calix[6]arenes that have been investigated in the present study indicates that modest changes in molecular structure can have a significant influence on the permeation properties of corresponding LB films. Most importantly, the need for strong intermolecular interactions within the assembly to minimize defect formation appears to be of primary impor-

(20) Langmuir, I. *J. Am. Chem. Soc.* **1917**, *39*, 1848.

tance. Thus, the strong cohesiveness of monolayers of **IV** can be directly correlated with its high He/N<sub>2</sub> selectivity in the form of an LB film. Judging from its cohesiveness, it would also appear that closure of the calix[6]arene pores through intramolecular hydrophobic interactions of the alkyl chains is unlikely and that intermolecular forces are dominant. Finally, it should be noted that defining the precise pore structure within these calix[6]arene-based LB films remains as one of the most challenging aspects that lies ahead. The principal uncertainties that await clarification are (i) the registry of the calix[6]arene pores between the layers (i.e., whether or not they align themselves to produce contiguous channels), (ii) the contributions that transient gaps between the calix[6]arenes make to the overall pore structure, and (iii) the presence or absence of residual defects.

## Conclusions

**Bridging the Gaps of a Support with Surfactant Monolayers Is Unlikely To Produce Defect-Free LB Films Unless Individual Surfactants Can Span Individual Pores.** The results of this study have shown that LB films derived from calix[6]arene-based surfactants as well as poly(1-octadecene-co-maleic anhydride) (**POM**), when supported on poly[1-(trimethylsilyl)-1-propyne] (**PTMSP**) cast film, possess permeation selectivities that *are not* dominated by defects. In contrast, those LB films that were assembled from conventional single-chain surfactants showed no significant permeation selectivity and appeared to undergo spontaneous disassembly. These striking differences have been found to correlate with the surfactant's ability to remain at the surface of **PTMSP**; i.e., only those surfactants that can span individual pores of **PTMSP** remain on its surface and lead to permeation-selective membranes. We conclude, therefore, that it will be difficult if not

impossible to create relatively defect-free LB films that rely upon intermolecular association to bridge gaps on the surface of a support. Our presumption is that most of the failures that have been reported in the literature in forming defect-free LB films, in combination with macroporous supports, are due to this bridging problem.

**Strong Attractive Forces between Nearest Neighbors Helps To Minimize Defect Formation within Polymer-Supported LB Films.** Comparison of the permeation properties of the series of calix[6]arene-based LB films reported herein has shown that modest changes in molecular structure can have a significant influence on the permeation properties of corresponding LB films. In particular, our results have shown that by strengthening the attractive van der Waals forces between the calix[6]arenes through elongation of the alkyl chains, defect formation within these LB assemblies can be minimized.

Calix[6]arene-based LB composites, of the type reported herein, represent the thinnest membranes that have been fabricated to date for gas separations. A single bilayer of **II**, for example, represents a maximum film thickness of only 38 Å. The fact that the flux of a permeant across a membrane is inversely proportional to the membrane's thickness strongly suggests that LB films such as these should have considerable potential as high performance membranes that are capable of extraordinarily high throughputs and high permeation selectivities. Efforts aimed at exploring such possibilities are continuing in our laboratories.

**Acknowledgment.** We are grateful to the Division of Basic Energy Sciences and the Department of Energy (DE-FG02-85ER-13403) for support of this research.

JA970980W